Combined Natural-Convection and Radiation Heat Transfer Over an Isothermal Vertical Plate Embedded in a Porous Medium

Kouichi.Kamiuto* and Toshihiro.Iyama*

The present study examines the effects of thermal radiation on the non-Darcian natural convection over an isothermal vertical plate embedded in a porous medium. It is shown that, when radiation effects are taken into account in the analysis, the resultant heat transfer characteristics increases with the temperature of a heated plate.

Key words : Porous media, natural convection, radiation, vertical plate, Nusselt number

1.Introduction

Natural convection in porous media has received much attention in several areas including geophysics, thermal insulation engineering and chemical reactor engineering, and a large number of reports have been accumulated in the past few decades. Earlier analytical studies of natural convection in porous media (Masuoka, 1968; Cheng and Minkowycz, 1977) have been based on Darcy's law with boundary friction and inertial effects neglected, but recent analyses have included these effects, together with nonuniform porosity effect (Hong, Yamada and Tien, 1987) and have clarified the validating regions of previous heat transfer correlations quantitatively (Evans and Plumb, 1978; Cheng, 1987). However, the effects of thermal radiation on natural convection heat transfer in porous media have not yet been examined in these previous literatures.

The purpose of the present study is to circumvent this deficiency. To this end, simultaneous natural-convection and correlated-radiation heat transfer over a vertical flat-plate with an isothermal wall temperature T_W embedded in a gas-filled packed bed with temperature T_∞ is analysed theoretically utilizing a finite-difference scheme. Although variable-porosity and boundary friction effects are disregarded in the analysis, the porous inertial term (Forchheimer term) in the momentum equation is taken into account. Moreover, radiative transfer within a porous medium is analysed utilizing correlated-radiative properties of packed spheres (Kamiuto, 1992; Kamiuto and San San Yee, 2005) and the P_1 approximation to the equation of transfer (Kamiuto, Saito and Ito, 1992).

Received on January 31, 2006

*Deparment of Mechanical and Energy Systems Engineering, Oita University,

2.Governing Equations

Under the assumptions that the porosity within a porous medium is uniform and the Boussinesque apporoximation is applicable, the governing equations with boundary friction, convection, inertia and thermal dispersion effects neglected are

$$\partial u/\partial x + \partial v/\partial y = 0, \tag{1}$$

$$(\mu/K)u + \rho_f C u^2 = g\,\rho_f \beta (T - T_\infty), \tag{2}$$

$$\rho_f\, C_{pf}(u\partial T/\partial x + v\partial T/\partial y) = k_e(\partial^2 T/\partial Y^2) - div\,\vec{q}_R, \tag{3}$$

$$div\,\vec{q}_R = \sigma_a(4\sigma T^4 - G). \tag{4}$$

Here, the coordinate along the hot boundary is denoted by x and that perpendicular to it is described by y, and u and v, respectively, represent the velocity components in the x and y directions.

K and C are the permeability and the inertial coefficient of a porous medium and are represented by

$$K = d_p{}^2\phi^3 / 150(1-\phi)^2, \tag{5}$$

$$C = 1.75(1-\phi)/d_p\phi^3. \tag{6}$$

The boundary conditions for Eqs. (1) to (3) are

$$\left.\begin{aligned} &y = 0 : v = 0, \quad T = T_w. \\ &y \to \infty : u = v = 0, \quad T = T_\infty. \end{aligned}\right\} \tag{7}$$

Moreover, since Eq. (3) involves the incident radiation defined by $2\pi \int_{-1}^{1} I(y,\xi)d\xi$, the equation of transfer governing the intensity of radiation I(y, ξ) must also be solved, together with Eqs. (1) to (3). In the present study, we utilize the first-order spherical harmonic method (P_1 approximation) to solve the equation of transfer because this approximation has been proved to be valid as long as the optical thickness of a medium is sufficiently large (Harris, 1989): this is the case for almost all packed-bed heat transfer problems.

The P_1 equations are written as:

$$dq_r / dy + \beta(1-\omega)G = 4\beta(1-\omega)\sigma T^4, \tag{8}$$

$$dG/dy + 3\beta(1-\omega\tilde{g})q_r = 0. \tag{9}$$

These equations are subject to the following boundary conditions:

$$\left.\begin{aligned} &y=0: \varepsilon_w G(0)/2 + (2-\varepsilon_w)q_r(0) = 2\varepsilon_w \sigma T_w^4, \\ &y\to\infty: dG/dy = 0 \quad (or \quad q_r = 0). \end{aligned}\right\} \tag{10}$$

With our correlated-scattering theory (Kamiuto, 1992; Kamiuto and San San Yee, 2005), the radiative properties such as β, ω and $\tilde{g}$ appearing in Eqs. (8) and (9) may be written as

$$\left.\begin{aligned} &\beta = (2\gamma_2 - 1)(\pi d_p^2 n_p / 4), \\ &\omega = \rho_s, \\ &\tilde{g} = -4/9, \\ &\gamma_2 = 1 + 1.5(1-\phi) - (3/4)(1-\phi)^2, \end{aligned}\right\} \tag{11}$$

where γ_2 represents the extinction-enhancement factor.

3.Dimensionless Governing Equations

We introduce the following dimensionless quantities to rewrite the governing equations in dimensionless form:

$$\left.\begin{aligned} &Da = K/x_0^2, \quad Fh = Cx_0, \quad \hat{G}r = g\beta\Delta TCK^2/\nu^2, \\ &N_R = k_e / 4\sigma T_W^3 x_0, \ \mathrm{Pr} = \mu c_{Pf} / k_f, \\ &Ra = g\beta\Delta T x_0^3 / \nu^2, \quad \hat{R}ad = \rho_f c_{pf} g\beta\Delta T x_0 K / k_e \nu, \\ &u^* = u/(Kg\rho_f\beta\Delta T/\mu), \\ &v^* = v/(Kg\rho_f\beta\Delta T/\mu), \quad x^* = x/x_0, \\ &y^* = y/x_0, \quad \Gamma = x_0/d_p, \\ &\theta = (T-T_\infty)/(T_W - T_\infty), \\ &\theta_\infty = T_\infty / T_W, \lambda_m = k_e / k_f, \\ &\tau_0 = \beta\cdot x_0 = 1.5\Gamma(2\gamma_2 - 1)(1-\phi), \\ &\chi = G/\sigma T_W^4, \quad \psi = q_r x_0 / k_e T_W, \end{aligned}\right\} \tag{12}$$

where $\hat{G}r$ represents the modified Grashof number, $\hat{R}ad$ the Darcy-Rayleigh number and these quantities may be rewritten as

$$\left.\begin{aligned} &\hat{G}r = RaDa^2 Fh, \\ &\hat{R}ad = RaDa\,\mathrm{Pr}/\lambda_m. \end{aligned}\right\} \tag{13}$$

Introducting these variables yields the governing equations of the form:

$$\partial u^*/\partial x^* + \partial v^*/\partial y^* = 0, \tag{14}$$

$$u^* + \hat{G}_r u^{*2} = \theta, \tag{15}$$

$$\begin{aligned} &u^*(\partial\theta/\partial x^*) + v^*(\partial\theta/\partial y^*) = \\ &(1/\hat{R}ad)\partial\theta^2/\partial y^{*2} - \left[\tau_0(1-\omega)/N_R\hat{R}ad(1-\theta_\infty)\right] \\ &\times\left[\{(1-\theta_\infty)\theta + \theta_\infty\}^4 - \chi/4\right] . \end{aligned} \tag{16}$$

The relevant boundary conditions can be rewritten as

$$\left.\begin{aligned} &y^* = 0 : v^* = 0, \qquad \theta = 1, \\ &y^* \to \infty : u^* = v^* = 0, \qquad \theta = 0. \end{aligned}\right\} \tag{17}$$

The P_1 equations may also be rewritten in dimensionless form:

$$\begin{aligned} &d\psi/dy^* + \{\tau_0(1-\omega)/4N_R\}\chi \\ &= \{\tau_0(1-\omega)/N_R\}\{(1-\theta_\infty)\theta + \theta_\infty\}^4, \end{aligned} \tag{18}$$

$$d\chi/dy^* + 12\tau_0(1-\omega\tilde{g})N_R\psi = 0. \tag{19}$$

The corresponding boundary conditions are

$$\left.\begin{aligned} &y^*=0: \\ &\varepsilon_W\chi(0)/2-[(2-\varepsilon_W)/3\tau_0(1-\omega\tilde{g})](d\chi/dy^*) \\ &\quad =2\varepsilon_W \\ &y^*\to\infty: \quad d\chi/dy^*=0 \end{aligned}\right\} \tag{20}$$

4.Variable Transformation

The continuity equation (14) may automatically be satisfied by introducing the stream function $\tilde{\psi}$:

$$\left.\begin{aligned} u^* &= \partial\tilde{\psi}/\partial y^*, \\ v^* &= -\partial\tilde{\psi}/\partial x^*. \end{aligned}\right\} \tag{21}$$

In addition, let us introduce the following variable transformations proposed by Masuoka (1968):

$$\tilde{\psi} = \sqrt{x^*/\hat{R}ad}\,\zeta(\eta), \tag{22}$$

$$\eta = y^*\sqrt{\hat{R}ad/x^*}. \tag{23}$$

Substitution of Eqs. (22) and (23) into Eqs. (15) and (16) yields

$$\zeta'(\eta) + \hat{G}r[\zeta'(\eta)]^2 = \theta(\eta), \tag{24}$$

$$\text{or} \quad \zeta'(\eta) = \left[-1+\sqrt{1+4\hat{G}r\theta(\eta)}\right]/2\hat{G}r \tag{25}$$

$$\left.\begin{aligned} &\zeta(\eta)\theta'(\eta)/2+\theta''(\eta) = \\ &\left[\tau_0(1-\omega)x^*/\hat{R}adN_R(1-\theta_\infty)\right] \\ &\times\left[\{(1-\theta_\infty)\theta+\theta_\infty\}^4-\chi(\eta)/4\right] \end{aligned}\right\} \tag{26}$$

which are subject to the following transformed boundary conditions:

$$\left.\begin{aligned} &\eta=0: \quad \zeta=0, \quad \theta=1, \\ &\eta\to\infty: \quad \zeta'=0, \quad \theta=0. \end{aligned}\right\} \tag{27}$$

The primes indicate differential with respect to η.

On the other hand, substitution of ψ obtained from Eq.(19) into Eq.(18) yields an ordinary differential equation of the second order with respect to χ:

$$\begin{aligned} &\chi'' - 3\tau_0^2(1-\omega)(1-\omega\tilde{g})(x^*/\hat{R}ad)\chi \\ &= -12\tau_0^2(1-\omega)(1-\omega\tilde{g})(x^*/\hat{R}ad)\theta^4. \end{aligned} \tag{28}$$

The boundary conditions for Eq. (28) are

$$\left.\begin{aligned} &\eta=0: \\ &\varepsilon_W\chi(0)/2-[(2-\varepsilon_W)/3\tau_0(1-\omega\tilde{g})] \\ &\quad\times\sqrt{\hat{R}ad/x^*}\,\chi'(0)=2\varepsilon_W, \\ &\eta\to\infty: \chi'=0. \end{aligned}\right\} \tag{29}$$

It should be noted that, when radiation is taken into account, the transformed energy equation depends not only on the similarity variable η but also on χ^*.

5.Heat Transfer Evaluation

The total heat flux at a heated plate is given by

$$\begin{aligned} q_t &= -k_e(\partial T/\partial y)|_{y=0} + q_r(0) \\ &= h(T_W - T_\infty), \end{aligned} \tag{30}$$

where h represents the local heat transfer coefficient.

The local Nusselt number may be defined as

$$\begin{aligned} Nu_x &= hx/k_e \\ &= \left[-\sqrt{\hat{R}ad\cdot x^*}\,\theta'(0)+\{x^*/(1-\theta_\infty)\}\psi(0)\right]. \end{aligned} \tag{31}$$

Rearranging Eq. (31) yields

$$\begin{aligned} &Nu_x/\sqrt{\hat{R}ad\cdot x^*} \\ &=\left[-\theta'(0)-\chi'(0)/\{12\tau_0(1-\omega\tilde{g})N_R(1-\theta_\infty)\}\right]. \end{aligned} \tag{32}$$

The mean Nusselt number over a heated plate can be evaluated as

$$\begin{aligned} Nu_m &= \int_0^1 (Nu_x/x^*)dx^* \\ &= \int_0^1 \sqrt{\hat{R}ad\cdot x^*}\,[-\theta'(0) \\ &\quad -\chi'(0)/\{12\tau_0(1-\omega\tilde{g})N_R(1-\theta_\infty)\}]dx^*. \end{aligned} \tag{33}$$

6.Numerical Methods

Governing equations (25) (26) and (28) were solved numerically using a finite-difference scheme: all derivatives with respect to η appearing in these equations were represented by a central-difference scheme and a region of η from 0 to 30 was divided into 5000 equally spaced increments for finite difference calculations. A simple recurrence relation between ζ (i) and ζ (i-1) can be derived from the discretized form for the momentum equation and consequently a value of ζ (i) at any lattice point may be evaluated readily from a value of ζ (i-1), provided that a temperature distribution is known in the righthand side of Eq. (25).

On the otherhand, finite difference equations for the energy equation or the P_1 equation constitute a set of simultaneous linear equations in the tridiagonal form and thus can be solved readily utilizing the band matrix method. Actual computations have been done according to the following procedures: First to obtain the first approximation to ζ (η_i) we assume a uniform temperature distribution such as θ =0. Utilizing thus determined values of ζ (η_i) and θ (η_i), we solved a set of simultaneous linear equations for χ (η_i).

Once values of χ (η_i) were obtained, the finite difference equations for θ (η_i) can be readily solved. Thereafter, the derived solution for θ (η_i) was utilized to obtain new solutions for ζ (η_i) and χ (η_i), and similar computations were performed until the following convergence criterion is satisfied:

$$\left|(\theta^{(n)} - \theta^{(n-1)})/\theta^{(n)}\right| < 10^{-3}, \qquad (34)$$

where the subscript n represents the nth iteration.

7.Range of Parameters used in Numerical Computations

Values of the system parameters such as θ_∞, $\hat{Gr}$, $\hat{Rad}$, N_R, τ_0, ω, and $\tilde{g}$ must be prescribed before numerical computations, but these parameters depend each other, and therefore they could not be specified arbitrary. In the present study, we assume a packed-sphere system consisting of 4MPa helium and 0.005m diameter ceramic spheres with k_s=1.05 (W/mK) and ρ_s=0.1. The spheres were assumed to be randomly-packed, and thus the porosity of a bed is 0.39. The length of a hot plate embedded in a bed was varied as 0.1, 0.5, 1.0 and 10 (m). Under these conditions, values of the Darcy number for the present system are less than 2.7×10^{-6}, and this justifys to disregard the boundary friction term in the momentum equation (Evans and Plumb, 1978). The hemispherical emissivity of a hot plate was assumed to be unity and a ratio of an ambient temperature to a plate temperature θ_∞ was kept at 0.9 for all the cases examined here. Values of physical properties of 4MPa helium such as ν, k_f and Pr were evaluated at a representative temperature T_r defined by T_W-0.38(T_W - T_∞) (K).

Dimensionless effective thermal conductivity of the packed bed was evaluated utilizing Bruggeman's theory (Kamiuto, 1990) and was given as

$$\lambda_m = k_e / k_f$$
$$= (\kappa - 1)\kappa^{1/3}\phi$$
$$\times \left[\sqrt[3]{(-1+\sqrt{A})/2} - \sqrt[3]{(1+\sqrt{A})/2}\right] + \kappa, \qquad (35)$$

where $A = 1+(4/27)\phi^3(\kappa-1)^3/\kappa^2$.

The range of the system parameters used in the present computations is summarized in

Table 1.

Table 1. Ranges of variables used in the present numerical computations.

T_W [K]	δ_R	$\hat{R}_{ad}$ r_0 [m] 0.1	0.5	1.0	10.0	N_R r_0 [m] 0.1	0.5	1.0	10.0
1000	5.956×10^{-3}	1.979	9.894	19.787	197.87	0.0311	0.00622	0.00311	0.000311
800	1.266×10^{-2}	3.825	19.122	38.245	382.45	0.0577	0.0115	0.00577	0.000577
600	3.303×10^{-2}	8.821	44.103	88.207	882.07	0.127	0.0254	0.0127	0.00127
400	1.254×10^{-1}	28.943	144.715	289.433	2894.33	0.391	0.0782	0.0391	0.00391

8.Results and Discussion

Computational results are summarized in Figs. 1 to 4. Results of velocity profiles are not shown here because the x* component of the velocity can be directly evaluated from a temperature distribution using Eq. (25). Here, it should be noted that $u^*=\xi'(\eta)$.

Figure 1 shows the effects of the dimensionless position x^* along a vertical plate on temperature distributions. The broken line in this figure corresponds to the temperature profile for the case without radiation. Temperature profiles evaluated under consideration of the effects of thermal radiation rise higher over an entire region of η than those without considering radiation. This is due to the fact that porous media can absorb thermal radiation emitted from the hot boundary and thus its temperature is lifted up. It is of interest to note that temperature profiles obtained by accounting for thermal radiation scarcely depend on the dimensionless position x^*.

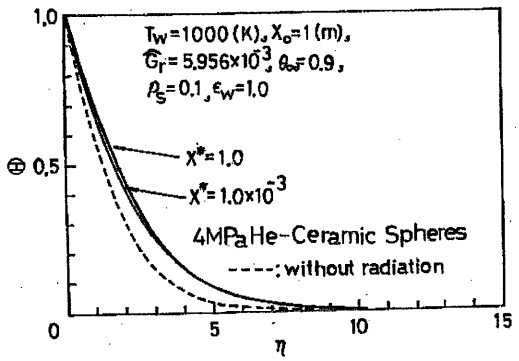

Fig.1. Effects of the dimensionless streamwise distance x^* on temperature distributions.

Figure 2 depicts the effects of a plate temperature T_W on temperature profiles of a porous medium at x*=0.5. Temperature profiles for pure convection depend on T_W through a temperature dependency of $\hat{Gr}$, but, as seen from this figure, this effect is quite negligible. Thus, the observed plate-temperature dependencies of a temperature distribution within a medium may be attributable to the effects of thermal radiation from a hot boundary: the radiation emitted from a hot boundary becomes larger as the boundary temperature rises higher.

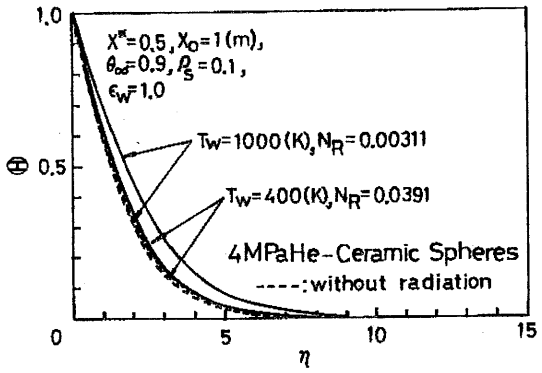

Fig.2. Effects of a heated plate temperature T_W on temperature distributions.

Variations in $Nu_x/\sqrt{\hat{Rad}\cdot x^*}$ against x^* is depicted in Fig. 3 for different values of T_W. As expected, the local Nusselt number increases with T_W. The result of pure Darcian natural-convection $(\hat{Gr}=0)$ is shown by the broken line, corresponding to $Nu_x/\sqrt{\hat{Rad}\cdot x^*}$ =0.4437 (Masuoka, 1968). The present numerical results of $Nu_x/\sqrt{\hat{Rad}\cdot x^*}$ for pure natural-convection accounting for the Forchheimer term in the momentum equation vary from 0.4383 to 0.4424, corresponding to the boundary temperature of 600～1000 [K]: The effects of the Forchheimer term on the heat transfer characteristics are comparatively small, and thus the difference observed between the broken line and the solid lines in this figure is due to the effects of radiation.

Figure 4 shows the relationship between the mean Nusselt number and $\hat{Rad}$. The broken line shows the theoretical results obtained by Masuoka (1968) for Darcian natural-convection over an isothermal vertical plate. The present results for pure natural convection

under consideration of the Forchheimer term are about 5% smaller, in the worst case, than that predicted from Masuoka's correlation, but, as seen from this figure, the difference between our result and Masuoka's correlation is quite negligible. The mean Nussselt number for non-Darcian natural-convection $(\hat{Gr} \neq 0)$ can be evaluated utilizing Pohlhausen's method and the resultant correlation may be written in the following form:

$$Nu_m = f(\hat{Gr})\sqrt{\hat{Rad}}\,, \tag{36}$$

$$f(\hat{Gr}) = [-(2/3)\cdot \hat{\mathrm{Gr}} + (4\hat{\mathrm{Gr}}+1)^{0.5} \times (8\hat{\mathrm{Gr}}+1)/16 - \{\ln(2\sqrt{\hat{\mathrm{Gr}}} + \sqrt{4\hat{\mathrm{Gr}}+1})\}/32\sqrt{\hat{\mathrm{Gr}}}]/\hat{\mathrm{Gr}} \tag{37}$$

This correlation is about 1.4% higher, in the worst case, than the exact numerical results. It can be seen from Fig.4 that the mean Nusselt number for the case considering radiation increases steadily with a plate temperature T_w and that, at T_w=1000 [K], Num is 30% higher than that for pure natural-convection.

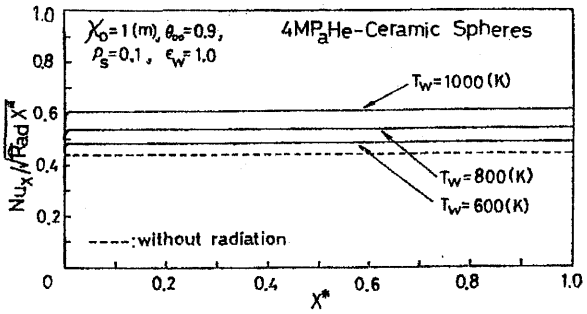

Fig.3. Variations in the local heat transfer parameter $Nu_x / \sqrt{\hat{Rad} \cdot x^*}$ along the x^* axis.

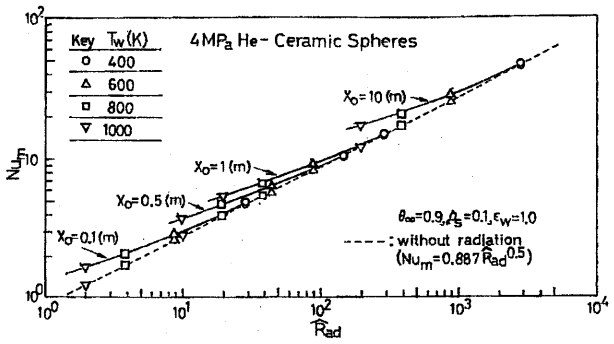

Fig.4. Relations between the mean Nusselt number and the Darcy-Rayleigh number.

9.Conclusions

The major conclusions that can be derived from the present study are summarized as follows:

1. Temperature distributions obtained under consideration of thermal radiation scarcely depend on the dimensionless position x* along a vertical heated plate.
2. Temperature distributions rise higher as a hot boundary temperature increases.
3. An analytical expression for the mean Nusselt number for pure non-Darcian natural convection Eq.(36), was dedrived.
4. The mean Nusselt number over a heated plate increases with a hot boundary temperature T_W, since heat transfer from a hot boundary at high temperatures is augmented by the presence of thermal radiation toward porous media. However, radiation did not affect the results by more than 30% even at T_W=1000 [K].

Nomenclature

C: inertial coefficient, Eq.(6)

C_p: specific heat of gas

Da: Darcy's number

D_p: particle diameter

Fh: Forchheimer coefficient

$f(\hat{Gr})$: a function of the modified Grashof number

G: incident radiation

$\hat{Gr}$: modified Grashof number

g: gravitational constant

$\tilde{g}$: asymmetry factor of the surface phase function of packed spheres

h: heat transfer coefficient

I(y, ξ): intensity of radiation

K: permeability, Eq.(5)

k_e: effective thermal conductivity of a packed bed

k_f: thermal conductivity of the continuous phase

k_s: thermal conductivity of the dispersed phase

N_R: conduction-radiation parameter

Nu_x: local Nusselt number

Nu_m: mean Nusselt number

n_p: number density of packed spheres

P_r: Prandtl number

$\overset{\cup}{q}_r$: radiative heat flux vector

q_r: cross-stream component of the radiative heat flux vector

q_t: total heat flux at the hot boundary

Ra: Rayleigh number

$\hat{Rad}$: Darcy-Rayleigh number

T: temperature

T_r: representative temperature

T_w: hot boundary temperature

T_∞: temperature at a distance from the hot boundary

u: velocity parallel to the hot boundary

x: streamwise coordinate

x_0: length of the hot boundary

y: cross-stream coordinate

β : coefficient of thermal expansion

Γ : dimensionless length of the hot boundary

γ_2: extinction-enhancement factor

ΔT : temperature difference($=T_w-T_\infty$)

ε_w: hemispherical emissivity of the hot boundary

η : dimensionless similarity variable

θ : dimensionless temperature

θ_∞: dimensionless temperature at a distance from the hot boundary

κ : a ratio of the thermal conductivity of solid to that of a fluid

λ m: dimensionless effective thermal conductivity of a packed bed

μ : fluid viscosity

ν : kinematic viscosity of a fluid

ξ : cosine of the angle between the normal to the hot boundary and the direction of propagation of radiation

ρ_f: density of a fluid

ρ_s: hemispherical reflectivity of packed spheres

σ : Stefan-Boltzmann's constant

σ_a: absrorption coefficient

τ_0: optical thickness

ϕ : mean porosity

χ : dimensionless incident radiation

ψ : dimensionless heat flux

$\tilde{\psi}$: dimensionless stream function

ω : albedo

Superscript

*:dimensionless quantity

References

Cheng, P. 1987. Wall effects on fluid flow and heat transfer in porous media. Proc. 2nd ASME/JSME Thermal Engng Joint Conf., Vol. 2, 297-303.

Cheng, P. and Minkowycz, W.J. 1977. Free convection about a vertical flat plate embedded in a porous medium with application to heat transfer from a dike. J Geophy. Res., 82, 2040-2044.

Evans, G.H. and Plumb, O.A. 1978. Natural convection from a vertical isothermal surface embedded in a saturated porous medium. ASME Paper No. 78-HT-55.

Harris, J.A. 1989. Solution of the conduction/radiation problem with linear-anisotropic scattering in an annular medium by the spherical harmonic method. L. Heat Transfer, 111, 194-197.

Hong, J.T., Yamada, Y. and Tien, C.L. 1987. Effects of non-Darcian and nonuniform porosity on vertical-plate natural convection in porous media. J. Heat Transfer, 109, 356-362.

Kamiuto, K. 1990. Examination of Bruggeman's theory for effective thermal conductivities of packed beds. J. Nucl. Sci. Techol., 27-5, 473-476.

Kamiuto, K. 1992. Radiative properties of packed-sphere systems estimated by the extended emerging-intensity fitting method. J.Quantita. Spectrosc. Radiat. Transfer, 47-4, 257-261.

Kamiuto, K., Saito, S. and Itoh, K. 1995. Numerical model for combined conduction and radiation heat transfer in annular packed beds. Numer. Heat Transfer, Part A, 28, 575-587.

Kamiuto, K. and San San Yee, 2005. Correlated radiative transfer through a packed bed of opaque spheres. Int. Commu. Heat Mass Transf., 32, 131-139.